Multi-$\bar{K}$ hypernuclei

D. Gazda,[1,*] E. Friedman,[2,†] A. Gal,[2,‡] and J. Mareš[1,§]
[1]*Nuclear Physics Institute, 25068 Řež, Czech Republic*
[2]*Racah Institute of Physics, The Hebrew University, Jerusalem 91904, Israel*
(Received 29 June 2009; published 25 September 2009)

Relativistic mean-field calculations of multi-$\bar{K}$ *hypernuclei* are performed by adding K^- mesons to particle-stable configurations of nucleons, Λ and Ξ hyperons. For a given hypernuclear core, the calculated $\bar{K}$ separation energy $B_{\bar{K}}$ saturates with the number of $\bar{K}$ mesons for more than roughly 10 mesons, with $B_{\bar{K}}$ bounded from above by 200 MeV. The associated baryonic densities saturate at values 2–3 times nuclear-matter density within a small region where the $\bar{K}$-meson densities peak, similarly to what was found for multi-$\bar{K}$ nuclei. The calculations demonstrate that particle-stable multistrange $\{N, \Lambda, \Xi\}$ configurations are stable against strong-interaction conversions $\Lambda \to N\bar{K}$ and $\Xi \to N\bar{K}\bar{K}$, confirming and strengthening the conclusion that kaon condensation is unlikely to occur in strong-interaction self-bound strange hadronic matter.

DOI: 10.1103/PhysRevC.80.035205 PACS number(s): 13.75.Jz, 21.65.Jk, 21.85.+d, 26.60.−c

I. INTRODUCTION

Quasibound nuclear states of $\bar{K}$ mesons have been studied by us recently in a series of articles [1–4], using a self-consistent extension of nuclear relativistic mean-field (RMF) models. References [1–3] focused on the widths expected for $\bar{K}$ quasibound states, particularly in the range of $\bar{K}$ separation energy $B_{\bar{K}} \sim 100$–150 MeV deemed relevant from K^--atom phenomenology [2,5] and from the KEK-PS E548 ^{12}C(K^-, N) missing-mass spectra [6] that suggest values of Re $V_{\bar{K}}(\rho_0) \sim -(150$–$200)$ MeV. Such deep potentials are not reproduced at present by chirally based approaches that yield values of Re $V_{\bar{K}}(\rho_0)$ of order -100 MeV or less attractive, as summarized recently in Ref. [7]. For a recent overview of $\bar{K}N$ and $\bar{K}$-nucleus dynamics, see Ref. [8].

The subject of multi-$\bar{K}$ nuclei was studied in Refs. [3,4], where the focal question considered was whether or not kaon condensation could occur in strong-interaction self-bound nuclear matter. Yamazaki *et al.* [9] argued that $\bar{K}$ mesons might provide the relevant physical degrees of freedom for reaching high-density self-bound strange matter that could then be realized as multi-$\bar{K}$ nuclear matter. This scenario requires that $B_{\bar{K}}$ beyond some threshold value of strangeness exceeds $m_K c^2 + \mu_N - m_\Lambda c^2 \gtrsim 320$ MeV, where μ_N is the nucleon chemical potential, thus allowing for the conversion $\Lambda \to \bar{K} + N$ in matter. For this strong $\bar{K}$ binding, Λ and Ξ hyperons would no longer combine with nucleons to compose the more conventional kaon-free form of strange hadronic matter, which is made out of $\{N, \Lambda, \Xi\}$ particle-stable configurations [10,11] (see Ref. [12] for an update), and $\bar{K}$ mesons would condense then macroscopically. However, our detailed calculations in Ref. [4] demonstrated a robust pattern of saturation for $B_{\bar{K}}$ and for nuclear densities upon increasing the number of $\bar{K}$ mesons embedded in the nuclear medium. For a wide range of phenomenologically allowed values of meson-field coupling constants compatible with assuming a deep $\bar{K}$-nucleus potential, the saturation values of $B_{\bar{K}}$ were found generally to be below 200 MeV, considerably short of the threshold value of $\approx$320 MeV required for the onset of kaon condensation under laboratory conditions. Similar results were subsequently published by Muto *et al.* [13]. Our discussion here concerns kaon condensation in self-bound systems, constrained by the strong interactions. It differs from discussions of kaon condensation in neutron stars where weak-interaction constraints are operative for any given value of density. For very recent works on kaon condensation in neutron-star matter, see Ref. [14], where hyperon degrees of freedom were disregarded, and Ref. [15], where the interplay between kaon condensation and hyperons was studied, and references to earlier relevant work cited therein.

In our calculations of multi-$\bar{K}$ nuclei [4], the saturation of $B_{\bar{K}}$ emerged for any boson-field composition that included the dominant vector ω-meson field, using the F-type SU(3) value $g_{\omega KK} \approx 3$ associated with the leading-order Tomozawa-Weinberg term of the meson-baryon effective Lagrangian. This value is smaller than in any of the other commonly used models [4]. Moreover, the contribution of each one of the vector ϕ-meson and ρ-meson fields was found to be substantially repulsive for systems with a large number of antikaons, reducing $B_{\bar{K}}$ as well as lowering the threshold value of the number of antikaons required for saturation to occur. We also verified that the saturation behavior of $B_{\bar{K}}$ is qualitatively independent of the RMF model applied to the nucleonic sector. The onset of saturation was found to depend on the atomic number. Generally, the heavier the nucleus is, the more antikaons it takes to saturate their separation energies. We concluded that $\bar{K}$ mesons do not provide a constituent degree of freedom for self-bound strange dense matter.

In the present work we extend our previous RMF calculations of multi-$\bar{K}$ nuclei into the domain of multi-$\bar{K}$ *hypernuclei*, to check whether a joint consideration of $\bar{K}$ mesons together with hyperons could bring new features or change our previous conclusions. This is the first RMF calculation that considers both $\bar{K}$ mesons and hyperons

*gazda@ujf.cas.cz
†elifried@vms.huji.ac.il
‡avragal@vms.huji.ac.il
§mares@ujf.cas.cz

 ©2009 The American Physical Society

together within *finite self-bound* hadronic configurations. The effect of hyperonic strangeness in bulk on the dispersion of kaons and antikaons was considered by Schaffner and Mishustin [16]. More recently, kaon-condensed hypernuclei as highly dense self-bound objects have been studied by Muto [17], using liquid-drop estimates.

The plan of the article is as follows. In Sec. II we briefly outline the RMF methodology for multi-$\bar{K}$ hypernuclei and discuss the hyperon and $\bar{K}$ couplings to the meson fields used in the present work. Results of these RMF calculations for multi-$\bar{K}$ hypernuclei are shown and discussed in Sec. III. We conclude with a brief summary and outlook in Sec. IV.

II. MODEL

A. RMF formalism

In the present work, our interest is primarily aimed at multiply strange baryonic systems containing (anti)kaons. We employed the relativistic mean-field approach where the strong interactions among pointlike hadrons are mediated by *effective* mesonic degrees of freedom. In the following calculations we started from the Lagrangian density

$$\begin{aligned}\mathcal{L} = {} & \bar{B}[i\gamma^\mu D_\mu - (M_B - g_{\sigma B}\sigma - g_{\sigma^* B}\sigma^*)]B + (D_\mu K)^\dagger (D^\mu K) \\ & - \left(m_K^2 - g_{\sigma K}\, m_K \sigma - g_{\sigma^* K}\, m_K \sigma^*\right) K^\dagger K \\ & + (\sigma, \sigma^*, \omega_\mu, \vec{\rho}_\mu, \phi_\mu, A_\mu \text{ free-field terms}) \\ & - U(\sigma) - V(\omega), \end{aligned} \tag{1}$$

which includes, in addition to the common isoscalar scalar (σ), isoscalar vector (ω), isovector vector (ρ), electromagnetic (A) fields, and nonlinear self-couplings $U(\sigma)$ and $V(\omega)$, also *hidden strangeness* isoscalar σ^* and ϕ fields that couple exclusively to strangeness degrees of freedom. Vector fields are coupled to baryons B (nucleons, hyperons) and K mesons via the covariant derivative

$$\begin{aligned} D_\mu = {} & \partial_\mu + i\, g_{\omega\Phi}\, \omega_\mu + i\, g_{\rho\Phi}\, \vec{I} \cdot \vec{\rho}_\mu + i\, g_{\phi\Phi}\, \phi_\mu \\ & + i\, e \left(I_3 + \tfrac{1}{2} Y\right) A_\mu \,, \end{aligned} \tag{2}$$

where $\Phi = B$ and K, with $\vec{I}$ denoting the isospin operator, I_3 being its z component, and Y standing for hypercharge. This particular choice of the coupling scheme for K^- mesons ensures the existence of a conserved Noether current, the timelike component of which can then be normalized to the number of K^- mesons in the medium,

$$\begin{aligned} & \rho_{K^-} = 2(E_{K^-} + g_{\omega K}\, \omega + g_{\rho K}\, \rho + g_{\phi K}\, \phi + e\, A) K^+ K^-, \\ & \int \mathrm{d}^3 x\, \rho_{K^-} = \kappa, \end{aligned} \tag{3}$$

and serves as a dynamical source in the equations of motion for the boson fields in matter:

$$\begin{aligned} \left(-\nabla^2 + m_\sigma^2\right)\sigma &= g_{\sigma B} \bar{B} B + g_{\sigma K} m_K K^+ K^- - \frac{\partial}{\partial \sigma} U(\sigma) \\ \left(-\nabla^2 + m_\sigma^{*2}\right)\sigma^* &= g_{\sigma^* B} \bar{B} B + g_{\sigma^* K} m_K K^+ K^- \\ \left(-\nabla^2 + m_\omega^2\right)\omega &= g_{\omega B} B^\dagger B - g_{\omega K} \rho_{K^-} + \frac{\partial}{\partial \omega} V(\omega) \\ \left(-\nabla^2 + m_\rho^2\right)\rho &= g_{\rho B} B^\dagger I_3 B - g_{\rho K} \rho_{K^-} \\ \left(-\nabla^2 + m_\phi^2\right)\phi &= g_{\phi B} B^\dagger B - g_{\phi K} \rho_{K^-} \\ -\nabla^2 A &= e\, B^\dagger \left(I_3 + \frac{1}{2} Y\right) B - e\, \rho_{K^-}. \end{aligned} \tag{4}$$

These *dynamically* generated intermediate fields then enter the Dirac equation for baryons,

$$\begin{aligned} & \left[-i\boldsymbol{\alpha} \cdot \boldsymbol{\nabla} + \beta\left(M_B - g_{\sigma B}\sigma - g_{\sigma^* B}\sigma^*\right) + g_{\omega B}\omega + g_{\rho B} I_3 \rho \right. \\ & \quad \left. + g_{\phi B}\phi + e\left(I_3 + \tfrac{1}{2} Y\right) A\right] B = \epsilon B, \end{aligned} \tag{5}$$

and the Klein-Gordon equation for K^- mesons,

$$\left[-\nabla^2 - E_{K^-}^2 + m_K^2 + \Pi_{K^-}\right] K^- = 0, \tag{6}$$

with the in-medium K^- self-energy,

$$\begin{aligned} \Pi_{K^-} = {} & -g_{\sigma K} m_K \sigma - g_{\sigma^* K} m_K \sigma^* \\ & - 2E_{K^-}(g_{\omega K}\omega + g_{\rho K}\rho + g_{\phi K}\phi + eA) \\ & - (g_{\omega K}\omega + g_{\rho K}\rho + g_{\phi K}\phi + eA)^2. \end{aligned} \tag{7}$$

Hence, the presence of the $\bar{K}$ mesons modifies the scalar and vector mean fields entering the Dirac equation, consequently leading to a *dynamical* rearrangement of the baryon configurations and densities that, in turn, modify the $\bar{K}$ quasibound states in the medium. This requires a self-consistent solution of these coupled wave equations, a procedure followed numerically in the present as well as in our previous works. In the present work, for the sake of simplicity, we have suppressed the imaginary part of Π_{K^-} arising from in-medium K^- absorption processes except for demonstrating its effect in one example. Note that, for the range of values $B_{K^-} \gtrsim 100$ MeV mostly considered here, the effect of Im Π_{K^-} was found to be negligible (see Fig. 1 of Ref. [4]).

B. Choice of the model parameters

To parametrize the nucleonic part of the Lagrangian density (1) we considered the standard RMF parameter sets NL-SH [18] and NL-TM1(2) [19], which have been successfully used in numerous calculations of various nuclear systems.

In the case of hyperons the coupling constants to the vector fields were fixed using SU(6) symmetry. For Λ hyperons this leads to

$$g_{\omega\Lambda} = \frac{2}{3} g_{\omega N}, \quad g_{\rho\Lambda} = 0, \quad g_{\phi\Lambda} = \frac{-\sqrt{2}}{3} g_{\omega N}. \tag{8}$$

The coupling to the scalar σ field, $g_{\sigma\Lambda}/g_{\sigma N} = 0.6184\,(0.623)$ for the NL-SH (NL-TM) RMF model, was then estimated by fitting to measured Λ-hypernuclear binding energies [20]. This essentially ensures the well depth of 28 MeV for Λ in nuclear matter. The coupling of the Λ hyperon to the scalar σ^* field was fixed by fitting to the measured value $\Delta B_{\Lambda\Lambda} \approx 1$ MeV of the uniquely identified hypernucleus ${}_{\Lambda\Lambda}{}^{6}$He [21]. For Ξ hyperons, SU(6) symmetry gives

$$g_{\omega\Xi} = \frac{1}{3} g_{\omega N}, \quad g_{\rho\Xi} = -g_{\rho N}, \quad g_{\phi\Xi} = -2\frac{\sqrt{2}}{3} g_{\omega N}. \tag{9}$$

Because there are no experimental data for $\Xi(\Lambda)$-Ξ interactions, we set $g_{\phi\Xi} = g_{\sigma^*\Xi} = 0$ to avoid parameters that might

TABLE I. $\bar{K}$ and K^- separation energies, $B_{\bar{K}}$ and B_{K^-}, respectively, calculated statically (in MeV) for a single antikaon $1s$ state in several nuclei, using the NL-TM nuclear RMF parametrizations (TM2 for ^{12}C and ^{16}O, TM1 for ^{40}Ca and above) and vector SU(3) coupling constants, Eq. (10). The difference $B_{K^-} - B_{\bar{K}}$ is due to the K^- finite-size Coulomb potential.

	^{12}C	^{16}O	^{40}Ca	^{90}Zr	^{208}Pb
$B_{\bar{K}}$	44.8	42.7	49.8	54.5	53.6
B_{K^-}	49.0	47.6	59.2	69.4	76.6

lead to unphysical consequences and that, in addition, are expected to play a minor role (in analogy to the small effect, of order 1 MeV for B_{K^-}, found upon putting $g_{\phi\Lambda}$ and $g_{\sigma^*\Lambda}$ to zero, and as is demonstrated below in Fig. 7 within a different context). The coupling to the scalar σ field was then constrained to yield an optical potential Re $V_{\Xi^-} = -14$ MeV in the center of ^{12}C [22]. This corresponds to $g_{\sigma\Xi} = 0.299 g_{\sigma N}$ for the NL-TM2 RMF model.

Finally, for the antikaon couplings to the vector meson fields we adopted a purely F-type, vector SU(3) symmetry:

$$2g_{\omega K} = 2g_{\rho K} = \sqrt{2}g_{\phi K} = g_{\rho\pi} = 6.04, \qquad (10)$$

where $g_{\rho\pi}$ is due to the $\rho \to 2\pi$ decay width [7]. (Here we denoted by g_{VP} the VPP electric coupling constant g_{VPP}.) Using this "minimal" set of coupling constants to establish correspondence with chirally based approaches, we calculate the single antikaon $1s$ separation energies $B_{\bar{K}}$ and B_{K^-} listed in Table I. These separation energies are lower roughly by 25 MeV than those anticipated from $\bar{K}N$-$\Sigma\pi$ coupled-channel chiral approaches [7], most likely because the $K^\star$ vector-meson off-diagonal coupling is not included in the standard RMF formulation. The missing attraction, and beyond it, is incorporated here by coupling the antikaon to scalar fields σ and σ^*. SU(3) symmetry is not of much help when fixing the coupling constants of scalar fields. Because there still is no consensus about the microscopic origin of the scalar σ field and the strength of its coupling to $\bar{K}$ mesons [23,24], in this work we fitted $g_{\sigma K}$ to several assumed K^- separation energies B_{K^-} in the range of 100–150 MeV for a single K^- meson in selected nuclei across the periodic table, as implied by the deep K^--nucleus potential phenomenology of Refs. [2,6]. Furthermore, for use in multistrange configurations, the coupling constant to the σ^* field is taken from $f_0(980) \to K\bar{K}$ decay to be $g_{\sigma^* K} = 2.65$ [16]. The effect of the σ^* field was found generally to be minor. For a more comprehensive discussion of the issue of scalar couplings, see our previous work [4].

C. Inclusion of the SU(3) baryon octet

We considered many-body systems consisting of the SU(3) octet N, Λ, Σ, and Ξ baryons that can be made particle stable against strong interactions [10,11]. The energy release Q values for various conversion reactions of the type $B_1 B_2 \to B_3 B_4$ together with phenomenological guidance on hyperon-nucleus interactions suggest that only the conversions $\Xi^- p \to \Lambda\Lambda$ and $\Xi^0 n \to \Lambda\Lambda$ (for which $Q \simeq 20$ MeV) can be overcome by binding effects. It becomes possible then to form particle-stable multi-$\{N, \Lambda, \Xi\}$ configurations for which the conversion $\Xi N \to \Lambda\Lambda$ is Pauli blocked owing to the Λ orbitals being filled up to the Fermi level. For composite configurations with Σ hyperons the energy release in the $\Sigma N \to \Lambda N$ conversion is too high ($Q \gtrsim 75$ MeV) and, hence, it is unlikely for hypernuclear systems with Σ hyperons to be particle stable.

III. RESULTS AND DISCUSSION

In Refs. [3,4] we studied multi-$\bar{K}$ nuclei, observing that the calculated K^- separation energies as well as the nuclear densities saturate upon increasing the number of K^- mesons embedded dynamically in the nuclear medium. This saturation phenomenon, which is qualitatively independent of the applied RMF model, emerged for any boson-field composition containing the dominant vector ω-meson field which acts repulsively between $\bar{K}$ mesons. Because the calculated K^- separation energies did not exceed 200 MeV, for coupling-constant combinations designed to bind a single K^- meson in the range $B_{K^-} \sim 100$–150 MeV, it was argued that kaon condensation is unlikely to occur in strong-interaction self-bound hadronic matter. In this section we demonstrate that these conclusions hold also when adding, within particle-stable multistrange configurations, large numbers of hyperons to nuclei across the periodic table.

A. Multi-$\{N, \Lambda, K^-\}$ configurations

Figure 1 presents $1s$ K^- separation energies B_{K^-} in $^{16}\mathrm{O} + \eta\Lambda + \kappa K^-$ multi-$K^-\Lambda$ hypernuclei as a function of the number κ of K^- mesons for $\eta = 0$, 2, 4, 6, and 8 Λ hyperons, calculated in the NL-SH model for two values of $g_{\sigma K}$ ($g_{\sigma K} = 0.233 g_{\sigma N}$ and $0.391 g_{\sigma N}$) chosen to produce $B_{K^-} = 100$ and 150 MeV, respectively, for $\eta = 0$, $\kappa = 1$. In addition, the lower group of curves with $B_{K^-} < 60$ MeV corresponds to $g_{\sigma K} = 0$. The figure illustrates saturation of B_{K^-} with the number of antikaons in multi-Λ hypernuclei. There is an apparent increase of B_{K^-} (up to 15%) when the first two Λ hyperons fill the $1s$ shell. Further Λ hyperons, placed in the p shell, cause only insignificant variation of B_{K^-} for small values of κ. However, the effect of the $1p_{3/2}$-shell hyperons increases with the number of antikaons, and for $\kappa = 8$ it adds another 5–10 MeV to B_{K^-}. The separation energy B_{K^-} remains almost unaffected (or even decreases) by the next two Λ hyperons placed in the $1p_{1/2}$ shell. The figure thus suggests saturation of the K^- separation energy also with the number η of Λ hyperons in the nuclear medium. When the K^- coupling to the σ field is switched off, $g_{\sigma K} = 0$, the K^- separation energy assumes relatively low values, $B_{K^-} \lesssim 50$ MeV, and decreases as a function of κ when Im Π_{K^-} is considered (solid lines). In this case, the effect of K^- absorption is not negligible as illustrated by the dot-dashed line showing B_{K^-} for Im $\Pi_{K^-} = 0$. The effect of Im $\Pi_{K^-} \neq 0$ for $B_{K^-} > 100$ MeV in the upper groups of curves is negligible and is not shown here or in all subsequent figures.

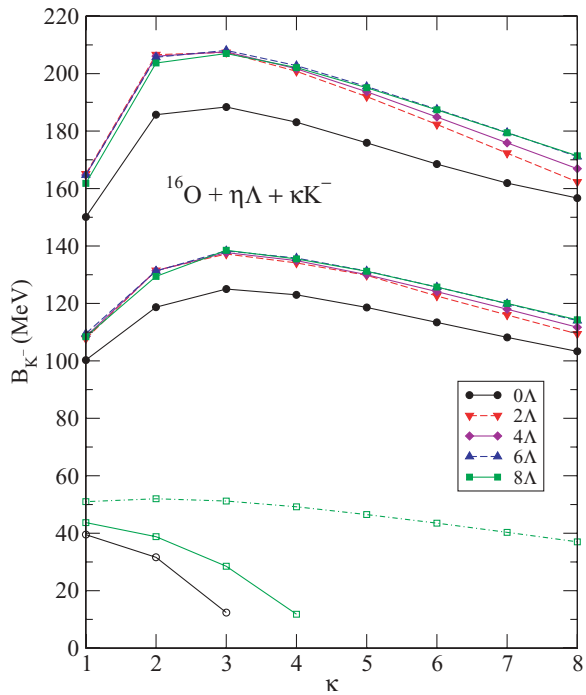

FIG. 1. (Color online) The $1s$ K^- separation energy B_{K^-} in ^{16}O + $\eta\Lambda + \kappa K^-$ as a function of the number κ of antikaons for several values of the number η of Λ hyperons, with initial values $B_{K^-} =$ 100 and 150 MeV for $\eta = 0$, $\kappa = 1$, calculated in the NL-SH RMF model. The solid (dot-dashed) lines with open symbols correspond to $g_{\sigma K} = 0$ including (excluding) Im Π_{K^-}.

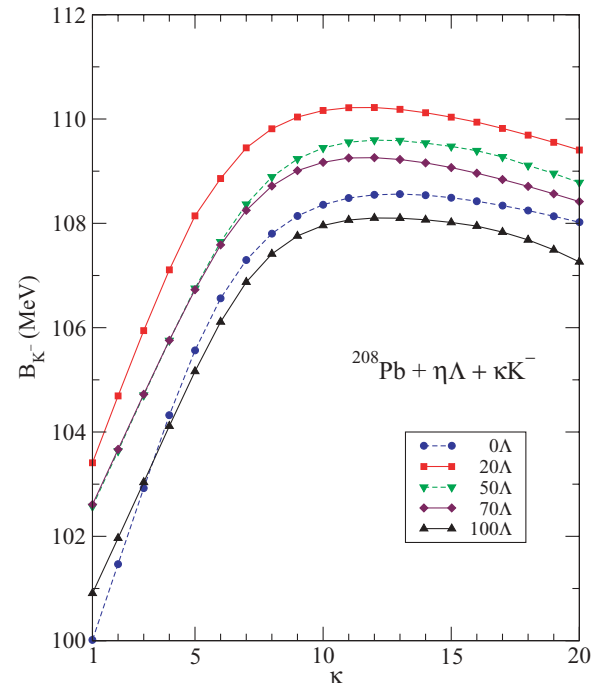

FIG. 2. (Color online) The $1s$ K^- separation energy B_{K^-} in ^{208}Pb + $\eta\Lambda + \kappa K^-$ as a function of the number κ of antikaons for several values of the number η of Λ hyperons, with initial value $B_{K^-} = 100$ MeV for $\eta = 0$, $\kappa = 1$, calculated in the NL-TM1 RMF model.

It is worth noting that $\eta = 8$ is the maximum number of Λ hyperons in our calculation that can be bound in the ^{16}O nuclear core. In some of the $^{16}\mathrm{O} + \eta\Lambda + \kappa K^-$ allowed configurtions, $1p_{1/2}$ neutrons became less bound than $1d_{5/2}$ neutrons because of the strong spin-orbit interaction. (This occurs, e.g., for $\eta = 0$ when $\kappa \geqslant 5$ or for $\eta = 8$ when $\kappa \geqslant 3$.) However, the total binding energy of the system was found always to be higher for configurations with $1p_{1/2}$ neutrons. Consequently, the standard shell configurations of oxygen are more bound and are thus energetically favorable.

The saturation of B_{K^-} upon increasing the number of Λ hyperons in multi-$K^-\Lambda$ hypernuclei based on a ^{16}O nuclear core holds also when going over to heavier core nuclei. Figure 2 shows the $1s$ K^- separation energy B_{K^-} in $^{208}\mathrm{Pb} + \eta\Lambda + \kappa K^-$ multi-$K^-\Lambda$ hypernuclei as a function of both the number κ of K^- mesons and η of Λ hyperons, calculated in the NL-TM1 model for $g_{\sigma K} = 0.133 g_{\sigma N}$ such that $B_{K^-} = 100$ MeV for $\eta = 0$, $\kappa = 1$. For any given number η of Λ hyperons, B_{K^-} saturates with the number κ of K^- mesons, reaching its maximum value for $\kappa = 12$. Morever, B_{K^-} increases with the number of hyperons up to $\eta = 20$, when it reaches its maximum value $B_{K^-} \approx 110$ MeV for $\kappa = 12$, and then starts to decrease with η. Consequently, in the Pb configurations with 100 Λ hyperons and more than 5 K^- mesons, K^- mesons are even less bound than in configurations with no Λ hyperons. The decrease of B_{K^-} with η beyond $\eta = 20$ is apparently related to a depletion of the central nuclear density in the presence of a massive number of hyperons in outer shells, as confirmed by some of the subsequent figures, because B_{K^-} is greatly affected by the central nuclear density.

B. Multi-{N, Λ, Ξ, K^-} configurations

When building up baryonic multi-{N, Λ, Ξ} configurations with maximum strangeness for selected core nuclei, we first started by filling up Λ hyperon single-particle states in a given nuclear core up to the Λ Fermi level. Subsequently, we added Ξ^0 and Ξ^- hyperons as long as the reaction $[AN, \eta\Lambda, \mu\Xi] \to [(A-1)N, \eta\Lambda, (\mu-1)\Xi] + 2\Lambda$ was energetically forbidden (here, [...] denotes a bound configuration). Finally, we checked that the inverse reaction $[AN, \eta\Lambda, \mu\Xi] \to [(A+1)N, (\eta-2)\Lambda, (\mu+1)\Xi]$ is kinematically blocked as well. These conditions guarantee that such {N, Λ, Ξ} multistrange configurations are particle stable against strong interactions, decaying only via weak interactions.

Clearly, the amount of Ξ hyperons bound in a given system depends on the depth $-V_\Xi$ of the Ξ-nucleus potential. We adopted a value for $g_{\sigma\Xi}$ that gives $V_\Xi^{\mathrm{Dirac}} = V_S + V_V = -18$ MeV, corresponding to a depth of $-V_\Xi^{\mathrm{Schr.}} \simeq 14$ MeV for use in the Schroedinger equation [22]. For comparison, in some cases we also considered $V_\Xi^{\mathrm{Dirac}} = -25$ MeV.

The ^{16}O core can accommodate up to $\eta = 8$ Λ hyperons in particle-stable configurations, and the $^{16}\mathrm{O} + 8\Lambda$ system admits many more, of order 40 K^- mesons. However, we have not found any energetically favorable conversion $\Lambda\Lambda \to \Xi N$ in $^{16}\mathrm{O} + \eta\Lambda + \kappa K^-$ systems. Therefore, Ξ hyperons are

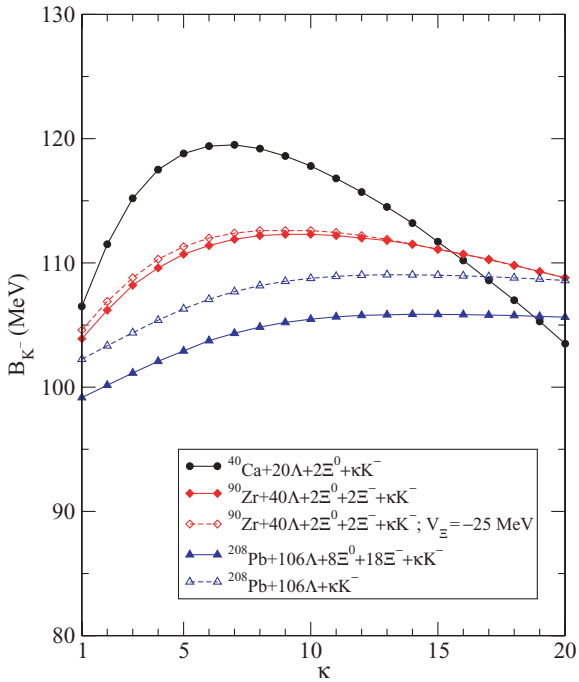

FIG. 3. (Color online) The 1s K^- separation energy B_{K^-} in ^{40}Ca, ^{90}Zr, and ^{208}Pb with $\eta\Lambda + \mu\Xi + \kappa K^-$ as a function of the number κ of antikaons, with initial value $B_{K^-} = 100$ MeV for $\eta = \mu = 0$, $\kappa = 1$, calculated in the NL-TM1 RMF model.

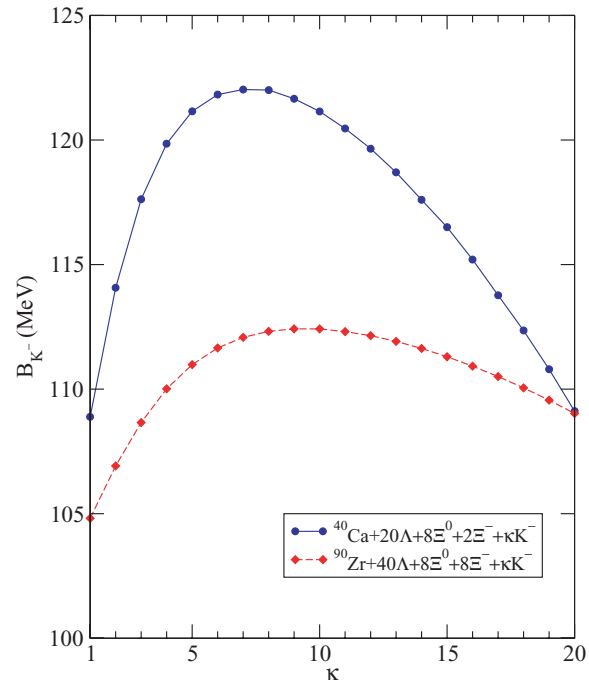

FIG. 4. (Color online) The 1s K^- separation energy B_{K^-} in ^{40}Ca and ^{90}Zr with $\eta\Lambda + \mu\Xi + \kappa K^-$, for $V_\Xi^{\rm Dirac} = -25$ MeV, as a function of the number κ of antikaons, with initial value $B_{K^-} = 100$ MeV for $\eta = \mu = 0$, $\kappa = 1$, calculated in the NL-TM1 RMF model.

not part of any particle-stable multistrange configurations built upon the ^{16}O core. While checking the energy balance in heavier systems with ^{40}Ca, ^{90}Zr, and ^{208}Pb nuclear cores, we found particle-stable configurations: $^{40}\mathrm{Ca} + 20\Lambda + 2\Xi^0$, $^{90}\mathrm{Zr} + 40\Lambda + 2\Xi^0 + 2\Xi^-$, and $^{208}\mathrm{Pb} + 106\Lambda + 8\Xi^0 + 18\Xi^-$. We then embedded several K^- mesons in these configurations and studied density distributions and binding energies in such multi-K^- hypernuclear systems. Figure 3 demonstrates the calculated 1s K^- separation energy B_{K^-} in $^{40}\mathrm{Ca} + 20\Lambda + 2\Xi^0 + \kappa K^-$, $^{90}\mathrm{Zr} + 40\Lambda + 2\Xi^0 + 2\Xi^- + \kappa K^-$, and $^{208}\mathrm{Pb} + 106\Lambda + 8\Xi^0 + 18\Xi^- + \kappa K^-$ as a function of the number κ of K^- mesons. For comparison, in the case of the ^{208}Pb core, we also present calculations done excluding Ξ hyperons but keeping the same number, $\eta = 106$, of Λ hyperons. A decrease of B_{K^-} upon adding hyperons (Ξ in this case) is noted, in line with the trend observed and discussed for Fig. 2 above.

The calculations shown in Fig. 3 were performed within the NL-TM1 nuclear RMF scheme using values of $g_{\sigma K} = 0.211 g_{\sigma N}$ (^{40}Ca) and $0.163 g_{\sigma N}$ (^{90}Zr), which yield $B_{K^-} = 100$ MeV for a single K^- nuclear configuration with $\eta = \mu = 0$, where μ denotes the number of Ξ hyperons. The figure demonstrates that the saturation of K^- separation energies, observed for multi-Λ hypernuclei in Figs. 1 and 2, holds also when Ξ hyperons are added dynamically within particle-stable configurations and that the heavier the system is, the larger number κ of antikaons it takes to saturate B_{K^-}. It is worth noting that in all cases B_{K^-} does not exceed 120 MeV. Finally, the two curves for a ^{90}Zr nuclear core in Fig. 3 (using diamond symbols) show the sensitivity to the value assumed for the Ξ hyperon potential depth, the standard $-V_\Xi^{\rm Dirac} = 18$ MeV, and a somewhat increased depth $-V_\Xi^{\rm Dirac} = 25$ MeV, illustrating the tiny effect it exercises on B_{K^-} that is noticeable only for $\kappa < 12$.

A deeper Ξ potential supports binding of more Ξ hyperons in a given multi-Λ hypernucleus. For $V_\Xi^{\rm Dirac} = -18$ MeV, only $2\Xi^0$ and $2\Xi^0 + 2\Xi^-$ hyperons were found to be bound in $^{40}\mathrm{Ca} + 20\Lambda$ and $^{90}\mathrm{Zr} + 40\Lambda$, respectively. However, for $V_\Xi^{\rm Dirac} = -25$ MeV it is possible to accommodate up to $8\Xi^0 + 2\Xi^-$ hyperons in $^{40}\mathrm{Ca} + 20\Lambda$ and $8\Xi^0 + 8\Xi^-$ hyperons in $^{90}\mathrm{Zr} + 40\Lambda$. Figure 4 presents the 1s K^- separation energy B_{K^-} in multi-K^- hypernuclei $^{40}\mathrm{Ca} + 20\Lambda + 8\Xi^0 + 2\Xi^- + \kappa K^-$ and $^{90}\mathrm{Zr} + 40\Lambda + 8\Xi^0 + 8\Xi^- + \kappa K^-$ as a function of the number κ of K^- mesons, calculated in the NL-TM1 model for $V_\Xi^{\rm Dirac} = -25$ MeV, using values for $g_{\sigma K}$ such that $B_{K^-} = 100$ MeV in $^{40}\mathrm{Ca} + 1K^-$ and in $^{90}\mathrm{Zr} + 1K^-$. The figure illustrates that the saturation of the K^- separation energy occurs also in baryonic systems with three species of hyperons, Λ, Ξ^0, and Ξ^-, reaching quite large fractions of strangeness [$|S|/B = 0.57(0.8)$ for a Ca(Zr) core]. We note that the separation energy B_{K^-} barely exceeds 120 MeV in these cases too.

We also studied the rearangement of nuclear systems induced by embedding hyperons and K^- mesons. Figure 5 presents the evolution of the density distributions in Zr after first adding $40\Lambda + 4\Xi$ hyperons (top panel) and then 10 K^- mesons (bottom panel). The nucleon density ρ_N in ^{90}Zr is denoted by a dotted line. The relatively weakly bound hyperons with extended density distributions (dashed line, solid diamonds) attract nucleons, thus depleting the

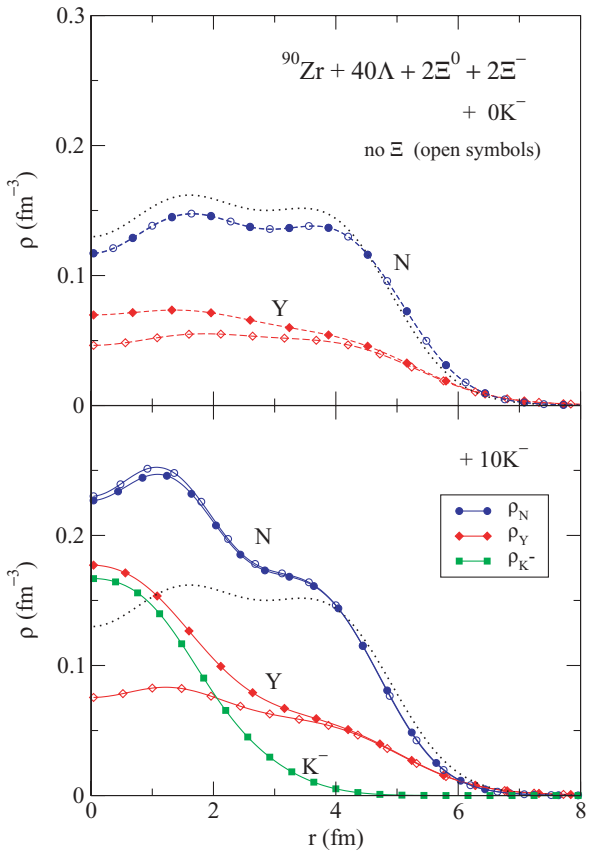

FIG. 5. (Color online) Density distributions in ^{90}Zr + 40Λ + $2\Xi^0 + 2\Xi^- + \kappa K^-$, for $\kappa = 0$ (top panel) and $\kappa = 10$ (bottom panel), with $B_{K^-} = 100$ MeV for $\eta = \mu = 0$, $\kappa = 1$, calculated in the NL-TM1 RMF model. The dotted line corresponds to the nucleon density ρ_N in ^{90}Zr. The densities ρ_Λ (open diamonds) and ρ_N (open circles) in ^{90}Zr + 40Λ + κK^- are shown for comparison.

central nucleon density ρ_N (dashed line, circles). Adding extra 10 K^- mesons to the hypernuclear system induces large rearrangement of the baryons. The K^- mesons, which pile up near the origin (solid line, squares), attract the surrounding nucleons and hyperons. Consequently, the densities ρ_N and ρ_Y (solid lines, solid circles and diamonds, respectively) increase considerably in the central region. The resulting configuration ^{90}Zr + 40Λ + $2\Xi^0 + 2\Xi^- + 10K^-$ is thus significantly compressed, with central baryon density ρ_B exceeding the nuclear density in ^{90}Zr by a factor of roughly 3.

For comparison we present in Fig. 5 also the Λ hyperon (ρ_Λ, open diamonds) and nucleon (ρ_N, open circles) density distributions calculated in ^{90}Zr + 40Λ + κK^- for $\kappa = 0$ and 10 K^- mesons. The removal of the 1s-state Ξ hyperons from the primary baryonic configuration ^{90}Zr + 40Λ + $2\Xi^0 + 2\Xi^-$ affects considerably the hyperon density distribution ρ_Y in the central region of the nucleus, this effect being magnified by the presence of K^- mesons. In contrast, the nucleon density ρ_N remains almost intact. For $\kappa = 10$, Ξ hyperons appear to repel nucleons from the center of the multi-$\{N, Y, \bar{K}\}$ system, much like Λ hyperons do.

C. Multi-$\{N, \Lambda, \Xi, K^+\}$ configurations

The K^+-nucleus potential is known to be repulsive, with $V_{K^+} \approx 30$ MeV at central nuclear density [5]. Schaffner and Mishustin [16] suggested that the presence of hyperons could lead eventually to a decrease of the repulsion that K^+ mesons undergo in nuclear matter so that the K^+ potential might even become attractive. Here we studied the possibility of binding K^+ mesons in hypernuclear matter, neglecting for simplicity dynamical effects arising from coupling K^+ mesons to the hypernuclear system. The K^+-nucleus potential was constructed simply by applying a G-parity transformation to the corresponding K^- potential, choosing $g_{\sigma K}$ such that it produces $B_{K^-} = 100$ MeV in the given core nucleus.

Figure 6 shows the radial dependence of the real part of the static K^+ potential in various hypernuclear systems connected with ^{16}O. The dotted line shows the repulsive K^+ potential in ^{16}O for comparison. The figure indeed shows that the repulsion decreases, from roughly 30 MeV down to roughly 20 MeV with the number of Λ hyperons added to the nuclear core, but the K^+ potential remains always repulsive in ^{16}O + $\eta\Lambda$ systems. Searching for a K^+ bound state in hadronic systems we also calculated the K^+ potential in more exotic multistrange hypernuclei ^{A}Z + $\eta\Lambda - \nu p$, where several protons are removed from the nuclear core in an attempt to increase the $|S|/B$ ratio and to reduce Coulomb repulsion. Figure 6 indicates that such removal of protons from ^{16}O has a sizable effect on the shape of the K^+ potential, which may result in a shallow attractive pocket. However, the attraction is insufficient to bind a K^+ meson in these hadronic systems.

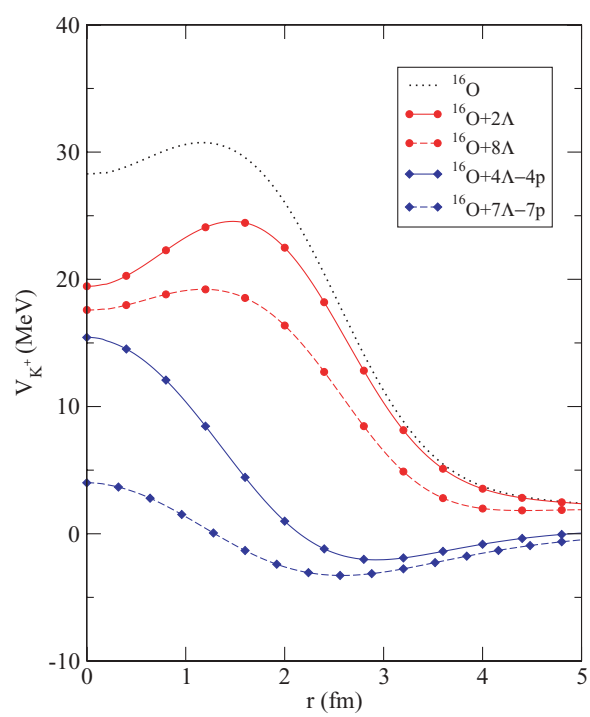

FIG. 6. (Color online) The K^+ static potential in ^{16}O + $\eta\Lambda - \nu p$, calculated in the NL-SH RMF model.

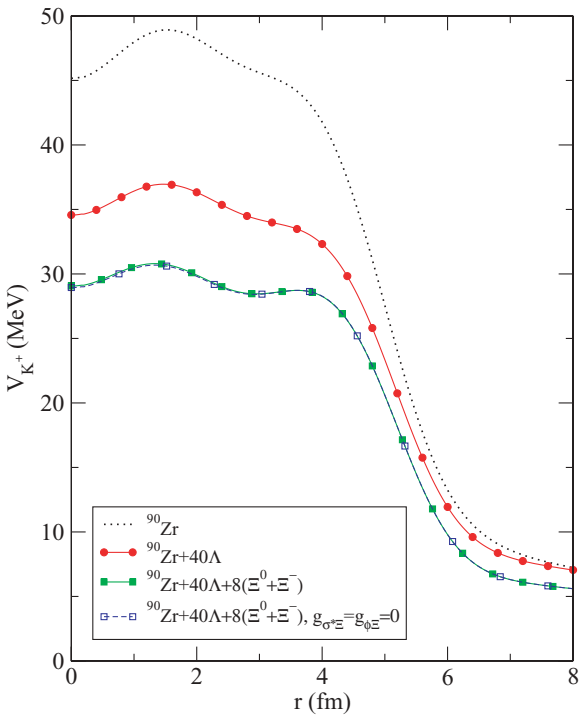

FIG. 7. (Color online) The K^+ static potential in $^{90}\mathrm{Zr} + \eta\Lambda + \mu(\Xi^0 + \Xi^-)$, calculated in the NL-TM1 RMF model.

Our calculations confirmed that the above conclusion holds also in heavier hypernuclear configurations based on Ca, Zr, and Pb cores.

In heavier nuclei, where it becomes possible to accommodate also Ξ hyperons in addition to Λ hyperons, the K^+ repulsion may be further reduced. This is demonstrated in Fig. 7 for a ^{90}Zr nuclear core. However, this reduction is insufficient to reverse the repulsion into attraction. The figure also shows that the *hidden strangeness* couplings (chosen to be $g_{i\Xi} = 2g_{i\Lambda},\ i = \sigma^*,\ \phi$) have no effect whatsoever on the reduction accomplished by the presence of Ξ hyperons.

Finally, we searched for K^+ bound states in nuclei sustained by K^- mesons. The presence of deeply bound K^- mesons makes the K^+ potential immensely deep (more than 100 MeV in $^{16}\mathrm{O} + 8\mathrm{K}^-$). However, because the K^- mesons are concentrated at the very center of the nucleus, the K^+ potential is of a rather short range of about 1 fm. As a result, we found only very weakly bound K^+ states (by 1 MeV) in multi-$\{N, Y, K^-\}$ configurations. A more careful treatment of K^+K^- dynamics near threshold is necessary before coming to further conclusions, but our conclusion is not at odds with recent studies of the $I = 1/2,\ J^\pi = 1/2^+$ $K\bar{K}N$ system [25,26].

IV. SUMMARY AND CONCLUSIONS

In this work, the RMF equations of motion for multi-$\bar{K}$ hypernuclei were formulated and solved for self-bound finite multistrange configurations. The choice of coupling constants of the constituents—nucleons, hyperons, and $\bar{K}$ mesons—to the vector and scalar meson fields was guided by a combination of accepted models and by phenomenology. The sensitivity to particular chosen values was studied. The results of the RMF calculations show a robust pattern of binding-energy saturation for $\bar{K}$ mesons as a function of their number κ. Compared to our previous RMF results for multi-$\bar{K}$ nuclei [4], the added hyperons do not bring about any quantitative change in the $B_{K^-}(\kappa)$ saturating curve. The main reason for saturation remains the repulsion induced by the vector meson fields, primarily ω, between $\bar{K}$ mesons. The $\mathrm{SU}(3)_V$ values adopted here for g_{vK}, Eq. (10), provide the "minimal" strength for $g_{\omega K}$ out of several other choices made in the literature, implying that the saturation of $B_{K^-}(\kappa)$ persists also for other choices of coupling-constant sets, as discussed in Ref. [4]. The repulsion between $\bar{K}$ mesons was also the primary reason for saturation in multi-$\bar{K}$ nuclei, both in our previous work [4] and in Ref. [13].

The saturation of B_{K^-} with typical values below 200 MeV, considerably short of what it takes to replace a Λ hyperon by a nucleon and a $\bar{K}$ meson, means that $\bar{K}$ mesons do not compete favorably and thus cannot replace hyperons as constituents of strange hadronic matter. In other words, $\bar{K}$ mesons do not condense in self-bound hadronic matter. The baryon densities of multi-$\bar{K}$ hypernuclei are between $2\rho_0$ and $3\rho_0$, where ρ_0 is nuclear-matter density. This is somewhat above the values obtained without $\bar{K}$ mesons, but still within the density range where hadronic models are likely to be applicable.

Our conclusion of no "kaon condensation" is specific to self-bound finite hadronic systems run under strong-interaction constraints. It is not directly related to the Kaplan-Nelson conjecture of macroscopic kaon condensation [27], nor to hadronic systems evolving subject to weak-interaction constraints, such as neutron stars. Yet, this conclusion has been challenged recently by Muto [17] who uses the liquid-drop approach to claim that multi-$\bar{K}$ hypernuclei (termed by him "kaon-condensed hypernuclei") may provide the ground-state configuration of finite strange hadronic systems at densities about $9\rho_0$. Of course this high value of density for kaon-condensed hypernuclei is beyond the range of applicability of hadronic models, because quark-gluon degrees of freedom must enter in this density range. His calculation also reveals an isomeric multistrange hypernuclear state, without $\bar{K}$ mesons, at density about $2\rho_0$ which is close to what we find here within a RMF bound-state calculation. The appearance of a high-density kaon-condensed hypernuclear bound state in Muto's calculation might be just an artifact of the applied liquid-drop methodology, which does not provide an accurate substitute for a more microscopically oriented bound-state calculation.

The role of K^- strong decays in hadronic matter was played down in the present calculation of multi-K^- hypernuclei because our aim, primarily, was to discuss and compare (real) binding energies of strange hadronic matter with and without K^- mesons. The width of deeply bound K^- nuclear configurations was explored by us in Refs. [1–3], concluding that residual widths of order $\Gamma_{K^-} \sim 50$ MeV due to $K^-NN \to \Lambda N, \Sigma N$ pionless conversion reactions are expected in the relevant range of binding energy $B_{K^-} \sim 100$–200 MeV. This estimate should hold also in multi-K^- hypernuclei where

added conversion channels are allowed: $K^-NY \to \Lambda Y$, ΣY, $K^-N\Lambda \to N\Xi$, and $K^-\Lambda Y \to \Xi Y$. We know of no physical mechanism capable of reducing substantially these widths, and therefore we do not anticipate multi-K^- nuclei or multi-K^- hypernuclei to exist as relatively long-lived isomeric states of strange hadronic matter that consists of multi-$\{N, \Lambda, \Xi\}$ configurations.

ACKNOWLEDGMENTS

This work was supported in part by GACR Grant 202/09/1441 and by SPHERE within the FP7 research grant system. AG acknowledges instructive discussions with Wolfram Weise and the support extended by the DFG Cluster of Excellence, Origin and Structure of the Universe, during a visit to the Technische Universität München.

[1] J. Mareš, E. Friedman, and A. Gal, Phys. Lett. **B606**, 295 (2005).
[2] J. Mareš, E. Friedman, and A. Gal, Nucl. Phys. **A770**, 84 (2006).
[3] D. Gazda, E. Friedman, A. Gal, and J. Mareš, Phys. Rev. C **76**, 055204 (2007).
[4] D. Gazda, E. Friedman, and A. Gal, J. Mareš, Phys. Rev. C **77**, 045206 (2008).
[5] E. Friedman and A. Gal, Phys. Rep. **452**, 89 (2007), and references to earlier work cited therein.
[6] T. Kishimoto *et al.*, Prog. Theor. Phys. **118**, 181 (2007); T. Kishimoto *et al.*, Nucl. Phys. **A827**, 321c (2009).
[7] W. Weise and R. Härtle, Nucl. Phys. **A804**, 173 (2008), and references to earlier work cited therein.
[8] A. Gal, Hyperfine Interact. (in press), arXiv:0812.0144 [nucl-th].
[9] T. Yamazaki, A. Doté, and Y. Akaishi, Phys. Lett. **B587**, 167 (2004).
[10] J. Schaffner, C. B. Dover, A. Gal, C. Greiner, and H. Stöcker, Phys. Rev. Lett. **71**, 1328 (1993).
[11] J. Schaffner, C. B. Dover, A. Gal, C. Greiner, D. J. Millener, and H. Stöcker, Ann. Phys. **235**, 35 (1994).
[12] J. Schaffner-Bielich and A. Gal, Phys. Rev. C **62**, 034311 (2000).
[13] T. Muto, T. Maruyama, and T. Tatsumi, Phys. Rev. C **79**, 035207 (2009).
[14] S. Banik, W. Greiner, and D. Bandyopadhyay, Phys. Rev. C **78**, 065804 (2008).
[15] T. Muto, Phys. Rev. C **77**, 015810 (2008).
[16] J. Schaffner and I. N. Mishustin, Phys. Rev. C **53**, 1416 (1996).
[17] T. Muto, Nucl. Phys. **A804**, 322 (2008).
[18] M. M. Sharma, M. A. Nagarajan, and P. Ring, Phys. Lett. **B312**, 377 (1993).
[19] Y. Sugahara and H. Toki, Nucl. Phys. **A579**, 557 (1994).
[20] O. Hashimoto and H. Tamura, Prog. Part. Nucl. Phys. **57**, 564 (2006).
[21] H. Takahashi *et al.*, Phys. Rev. Lett. **87**, 212502 (2001).
[22] P. Khaustov *et al.*, Phys. Rev. C **61**, 054603 (2000).
[23] A. Martinez Torres, K. P. Khemchandani, and E. Oset, Eur. Phys. J. A **36**, 211 (2008).
[24] R. Kamiński, G. Mennessier, and S. Narison, Phys. Lett B (in press), arXiv:0904.2555 [hep-ph].
[25] D. Jido and Y. Kanada En'yo, Phys. Rev. C **78**, 035203 (2008).
[26] A. Martinez Torres, K. P. Khemchandani, and E. Oset, Phys. Rev. C **79**, 065207 (2009); A. Martinez Torres, K. P. Khemchandani, U.-G. Meißner, and E. Oset, arXiv:0902.3633 [nucl-th].
[27] B. D. Kaplan and A. E. Nelson, Phys. Lett. **B175**, 57 (1986); **B179**, 409 (1986).